







Research Article

A DFT Mechanistic Study of the Regio-, Chemo-, and Stereo-Selectivities of the (3 + 2) Cycloaddition of Diarylnitrone Derivatives with 1-(4-Nitrophenyl)-5H-Pyrrolin-2-One

Sylvia Adomako ¹, Joshua Atta-Kumi ¹, Cecil H. Botchway ¹, Richard Tia ¹,
Evans Adei ¹ and Albert Aniagyei ²

¹Theoretical and Computational Chemistry Laboratory, Department of Chemistry,
Kwame Nkrumah University of Science and Technology, Kumasi, Ghana

²Department of Basic Sciences, University of Health and Allied Sciences, Ho, Ghana

Correspondence should be addressed to Albert Aniagyei; aanigyei@uhas.edu.gh

Received 16 December 2022; Revised 19 April 2023; Accepted 21 June 2023; Published 1 July 2023

Academic Editor: Arun Suneja

Copyright © 2023 Sylvia Adomako et al. This is an open access article distributed under the Creative Commons Attribution License, which permits unrestricted use, distribution, and reproduction in any medium, provided the original work is properly cited.

Heterocyclic compounds are vital in rational drug design by providing convenient means for the optimization of drugs or drug candidates. Isoxazolidine (a heterocyclic compound) derived from the (3 + 2) cycloaddition reaction is reported to possess anticancer, antiviral, antibacterial, and anti-inflammatory properties. The mechanistic study of the chemo-, regio-, and stereo-selectivities of the (3 + 2) cycloaddition reaction (32CA) of diarylnitrones (**A1**) to 1-(4-nitrophenyl)-5H-pyrrolin-2-one (**A2**) has been conducted using the density functional theory (DFT) method at the M06/6-311G (*d, p*) computational level. The 32CA reaction of **A1** and **A2** proceeds through a chemo-selective addition of **A1** across the C=C olefinic bond of **A2** to furnish both kinetically and thermodynamically favored reaction routes. The effect of substitution on the 32CA reaction has been studied using a representative set of electron-acceptor and electron-releasing groups on both **A1** and **A2**. The chemo-, regio-, and stereo-selectivities observed in the 32CA reaction remained unchanged irrespective of the substituents used on both reactants, but a change in kinetics and thermodynamics was observed based on the substituents. In the 32CA reaction of **A1** and **A2**, the “exo” cycloadduct formation was favored over the “endo” cycloadducts in all instances.

1. Introduction

Metal-mediated cycloadditions became unpopular compared to their metal-free processes because metals serve as a potential toxic waste source. However, metal-involving syntheses (particularly metal-catalysed reaction) are still preferred over relevant metal-free routes because metal centres could strongly activate reactants and/or substantially reduce the number of steps leading to target compounds [1–6].

For example, isoxazolidines (a heterocyclic compound) can be generated from the (3 + 2) cycloaddition (32CA) reaction, which involves the coupling of a three-atom component (TAC) and an ethylene derivative [7]. The 32CA reaction of nitrones to ethylene derivatives leads to the

generation of the isoxazolidine heterocyclic compounds, which possess anticancer, antiviral, antibacterial, and anti-inflammatory properties [8]. 5H-pyrrolin-2-ones, also known as 3-pyrrolin-2-ones, are nitrogen-containing heterocycles that can be derived from the oxidation of pyrroles [9]. Due to the reactive nature of this moiety, it is capable of undergoing reactions such as epoxidation [10, 11], cyclopropanation [12], and cycloaddition [13] reactions.

Langlois et al. [14] reported initial findings for the 32CA reaction of 5H-pyrrolin-2-ones with nitrones and stated that the reaction gave a mixture of stereoisomers and regioisomers which were separable by chromatography.

Muzychenko and coworkers [15] examined the 32CA reaction of diarylnitrone (**A1**) with 1-(4-nitrophenyl)-5H-

pyrrolin-2-one (**A2**) to produce 2-oxa-6-oxo-3-phenyl-4-(R-phenyl)-7-(4-nitrophenyl)-3,7-diazabicyclo (3,3.0) octane **1** as the major product (Scheme 1). It was reported that **A1** chemo-selectively added across the C=C olefinic bond of **A2** over the C=O functionality. Also, in the addition of **A1** across the C=C olefinic bond, it added regio-selectively across **A2** in an “exo” manner cis to the N-nitrophenyl group of **A2** to give a single isomeric product. Muzychenko and coworkers [15] reported that forming an “endo” approach is also plausible to be isolated in the reaction. From their experiment, it was concluded that different substituents on the nitrone gave different reaction times and product yields.

In this study, the regio-, chemo-, and stereo-selectivities and reaction mechanism of the 32CA of diarylnitrone derivatives (**A1**) with 1-(4-nitrophenyl)-5H-pyrrolin-2-one (**A2**) are elucidated. Path A observed experimentally by Muzychenko and coworkers [15] and plausible path B were considered in this study. We herein seek to determine the effect of electron-releasing groups (ERGs) and electron-acceptor groups (EAGs) by employing a wide range of substituents based on how strong, weak, or moderate the substituents are. Also, the effect of small and bulky groups on the reaction was explored. Understanding the factors controlling the reaction will help enhance chemical insights into the reaction. The study is based on Scheme 1 to depict the various regio- and stereo-selectivities involved in the reaction. The computed selectivities based on activation energies trends are then rationalized using local and global reactivity indices based on the conceptual DFT.

2. Computational Details and Methodology

Here, we present only a brief statement of the method because a fuller description is available in [16, 17]. The M06 hybrid functional [18] as implemented in Gaussian 09 [19] has been employed together with the split valence triple- ξ (TZ) basis set 6-311G (*d*, *p*) [20–22] in this study.

3. Results and Discussion

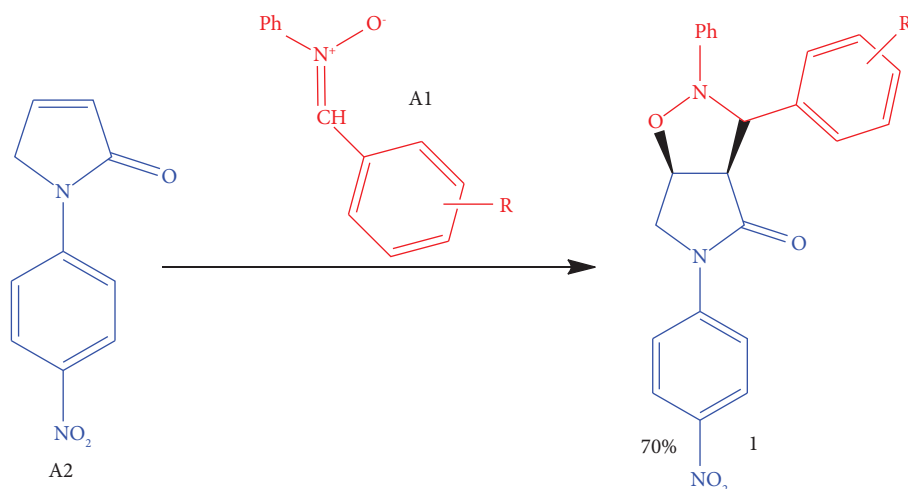
From Scheme 1, the mechanism of the 32CA reaction of diarylnitrone derivatives (**A1**) with 1-(4-nitrophenyl)-5H-pyrrolin-2-one (**A2**) is proposed to go through two different reaction pathways. 1-(4-nitrophenyl)-5H-pyrrolin-2-one (**A2**) has multiple reactive centres; therefore, diarylnitrone can add across its C=C olefinic bond in a (3 + 2) manner and similarly across the C=O bond. The zero-point corrected absolute energies and coordinates of all the computed structures reported herein are shown in Tables S1–S7 in the Supplementary file. The reaction path A from Scheme 1 emerges from the addition of **A1** across the C=C double bond of **A2** through transition states **TS1A-EXO**, **TS2A-ENDO**, **TS3A-EXO**, and **TS4A-ENDO** to furnish products **P1A-EXO**, **P2A-ENDO**, **P3A-EXO**, and **P4A-ENDO**, respectively. **P1A-EXO** and **P3A-EXO** result from the “exo” approach of **A1** with cis-stereospecific addition to the 1-(4-nitrophenyl)-5H-pyrrolin-2-one C=C olefinic bond. Products **P1A-EXO** and **P2A-ENDO** are stereoisomeric pairs,

likewise **P3A-EXO** and **P4A-ENDO**. Also, the pairs **P1A-EXO** and **P3A-EXO** and **P2A-ENDO** and **P4A-ENDO** are regioisomers.

Path B originates from the addition of **A1** across the C=O double bond of **A2** to afford **P1B** and **P2B** through their respective transition states, **TS1B** and **TS2B**. Product pairs **P1B** and **P2B** are regioisomers.

3.1. Analysis of the 32CA Parent Reaction of 1-(4-Nitrophenyl)-5H-Pyrrolin-2-One (A2) and Diarylnitrone (A1, R=H). This section provides mechanistic insights into the 32CA reaction of the diarylnitrone (**A1**, R=H) with 1-(4-nitrophenyl)-5H-pyrrolin-2-one (**A2**). The reported imaginary frequencies of the optimized transition states in the reaction of 1-(4-nitrophenyl)-5H-pyrrolin-2-one (**A2**) with diarylnitrone (**A1**, R=H) in gas phase at 25°C are presented in Tables S8. Figure 1 represents the Gibbs free energy profile for the 32CA reaction of **A2** and **A1** (R=H) in kcal/mol. Table 1 presents the calculated rate constants for the 32CA reaction of **A2** and **A1** (R=H) to furnish the cycloadducts. From Figure 1, the most preferred pathway is path A, which is associated with the chemo-selective addition of **A1** (R=H) across the C=C olefinic bond of **A2** to furnish the cycloadduct. Within path A, the formation of the “exo” product **P1A-EXO** (reaction energy of -22.2 kcal/mol) through **TS1A-EXO** (activation barrier of 4.5 kcal/mol) is the most kinetically favored reaction route with **P1A-EXO** being thermodynamically stable. The nearest competing pathway is the formation of **P4A-ENDO** (reaction energy of -20.3 kcal/mol) via the transition state **TS4A-ENDO** (activation barrier of 7.6 kcal/mol), where **TS1A-EXO** is kinetically favored by a difference of 3.1 kcal/mol. The cycloadduct **P1A-EXO** is irreversible since the reaction is highly exergonic due to its reaction energy. The lower activation barrier observed for **TS1A-EXO** and the thermodynamic stability of **P1A-EXO** correspond to the higher yield observed in the experiment. The endergonic cycloadducts found along path B, as a result of the addition of **A1** across the C=O functionality of the **A2** molecule via the transition states **TS1B** and **TS2B** with activation barriers of 13.0 kcal/mol and 51.5 kcal/mol, respectively, more than the most favorable transition state **TS1A-EXO**, were not isolated experimentally. The favored reaction route established in this study is in complete agreement with the experimental observation reported by Muzychenko et al. [15]. This indicates that the formation of **P1A-EXO** was a function of the step leading to it being kinetically favored over all other possible reaction channels or stages.

Table 1 shows the calculated rate constants for the formation of the isomeric cycloadducts considered in Scheme 2. As seen in Table 1, **P1A-EXO** has the highest rate constant of $3.1 \times 10^9 \text{ s}^{-1}$; this accounts for the greater yield observed experimentally. The closest competing pathway has a calculated rate constant of $1.7 \times 10^7 \text{ s}^{-1}$, making the formation of **P1A-EXO** about 182 times faster than the formation of **P4A-ENDO**, again confirming why the product **P1A-EXO** was isolated in a higher yield by Muzychenko et al. [15].



SCHEME 1: 32CA reaction of diarylnitrones (A1) with 1-(4-nitrophenyl)-5H-pyrrolin-2-one (A2).

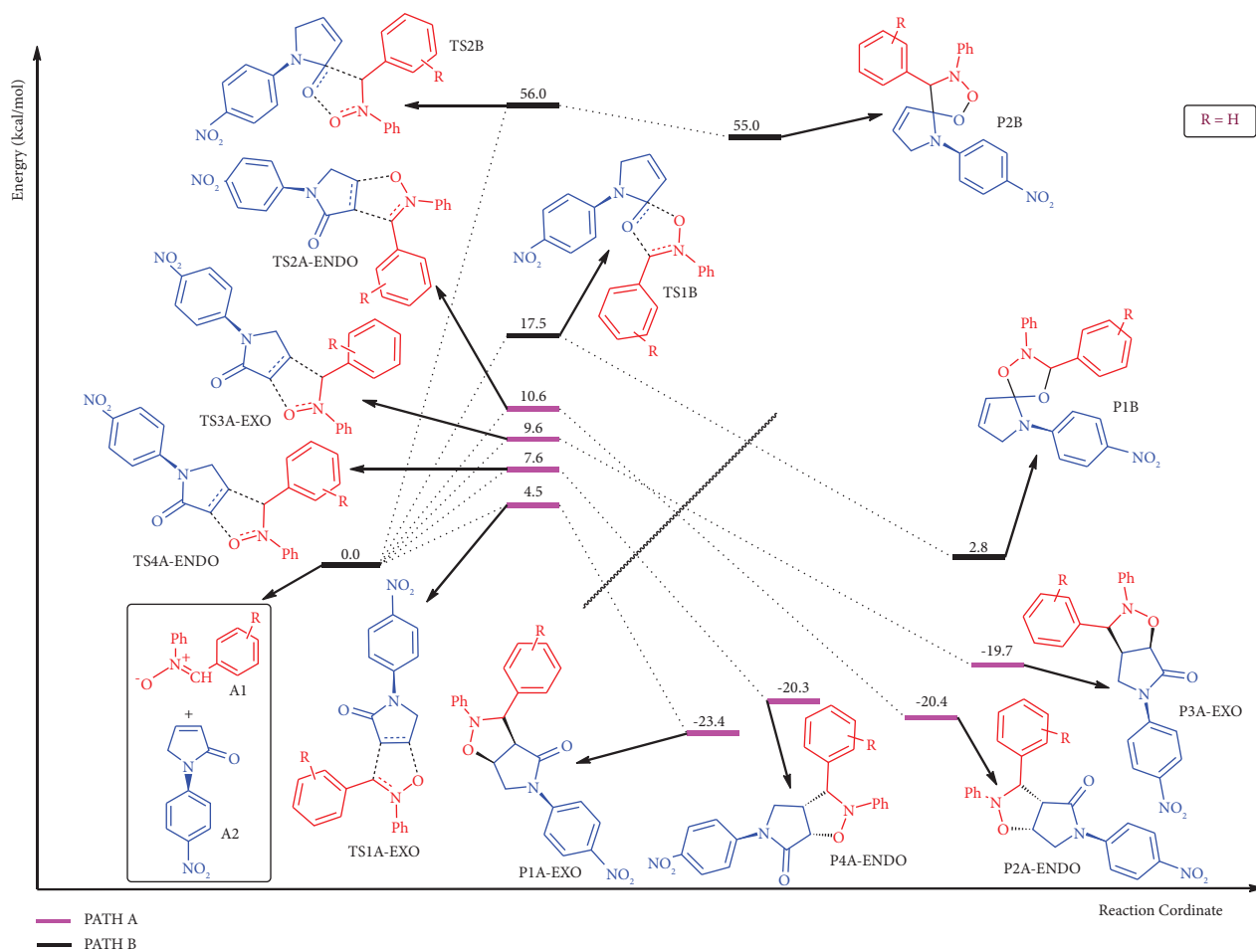


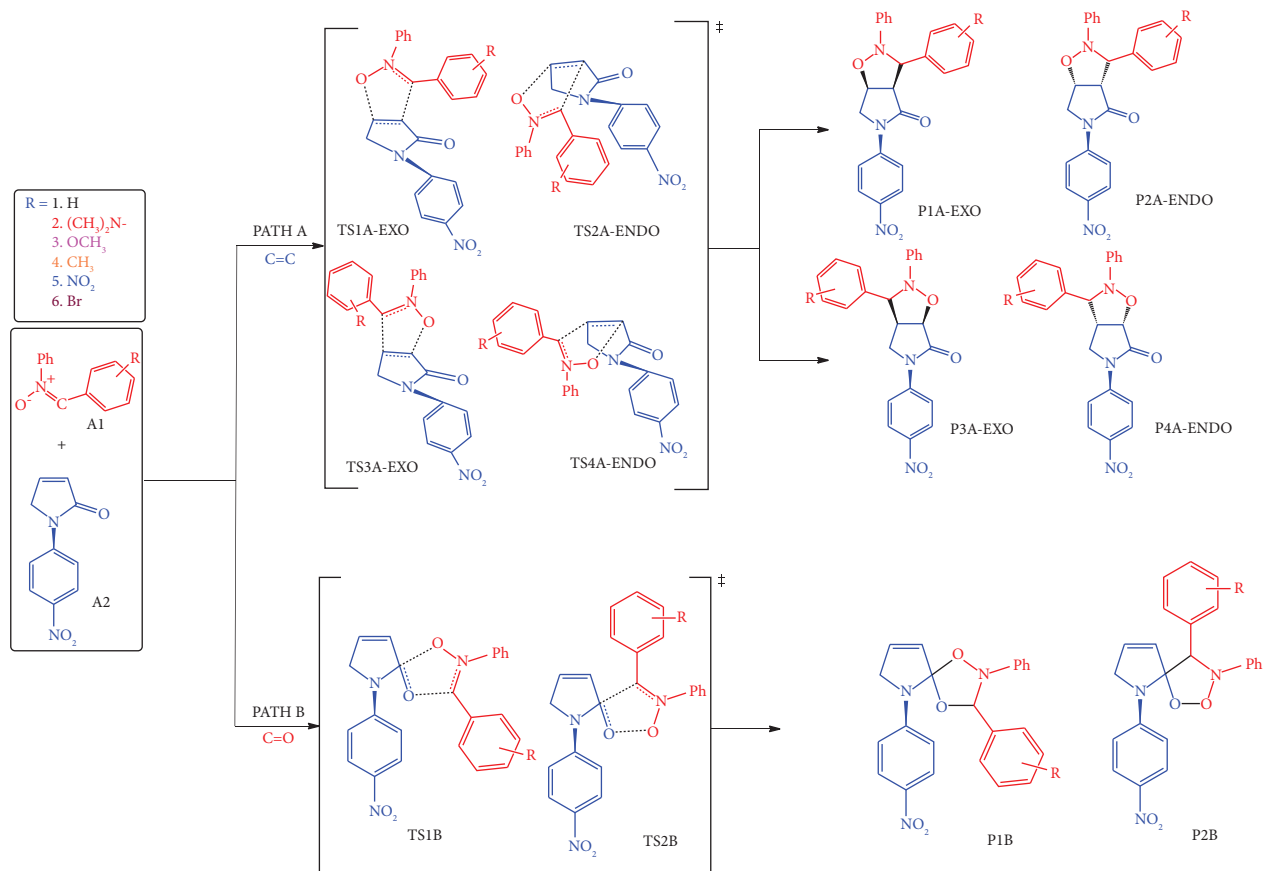
FIGURE 1: Gibbs free energy profile for the 32CA reaction of A1 (R=H) with A2 in the gas phase at the M06/6-311G (*d, p*) level of the theory.

3.2. *Effect of Substituents on the 32CA Reaction of 1-(4-Nitrophenyl)-5H-Pyrrolin-2-One (A2) and Diarylnitronone (A1, R = ERGs, and EAGs).* We report on the effect of electron-releasing groups (ERGs) and electron-acceptor groups (EAGs) at the meta and para positions of the aryl group of

the A1 molecule on the reaction. The activation and reaction energies of the transition states and products in the 32CA reaction of A1 (R = EAGs and ERGs) are displayed in Tables 2 and 3, respectively. Table 2 shows the substitution of the illustrative set of ERGs and EAGs at the para position,

TABLE 1: Rate constants (s^{-1}) at 25°C for the (3+2) cycloaddition reaction of diarylnitronone (**A1**, R=H) and 1-(4-nitrophenyl)-5H-pyrrolin-2-one (**A2**).

Products	Rate constants [$k(T)$]
P1A-EXO	3.1×10^9
P2A-ENDO	1.1×10^5
P3A-EXO	5.7×10^5
P4A-ENDO	1.7×10^7
P1B	9.2×10^{-1}
P2B	5.5×10^{-29}



SCHEME 2: Proposed scheme of study for 32CA reaction of diarylnitronones (**A1**) with 1-(4-nitrophenyl)-5H-pyrrolin-2-one (**A2**).

TABLE 2: Activation and reaction energies corresponding to transition states and products for the 32CA reaction of 1-(4-nitrophenyl)-5H-pyrrolin-2-one **A2** and **A1** (para, R=CH₃, OCH₃, (CH₃)₂N, Br, and NO₂) at the M06/6-311G (*d, p*) level of the theory in the gas phase for path A. All energies are in kcal/mol.

Substituents	Para							
	TS1A-EXO	TS2A-ENDO	TS3A-EXO	TS4A-ENDO	P1A-EXO	P2A-ENDO	P3A-EXO	P4A-ENDO
H	4.5	10.6	9.6	7.6	-23.4	-20.4	-19.7	-20.3
<i>ERGs</i>								
CH ₃	3.1	10.6	8.3	7.6	-23.5	-20.1	-19.5	-19.9
OCH ₃	9.2	17.9	14.7	15.5	-15.9	-12.1	-11.7	-12.1
(CH ₃) ₂ N	3.9	10.2	4.9	7.2	-24.2	-19.0	-18.3	-19.0
<i>EAGs</i>								
Br	4.2	11.2	9.8	8.2	-23.3	-19.8	-19.0	-19.8
NO ₂	5.1	12.0	15.6	9.2	-22.6	-19.6	-18.2	-19.2

TABLE 3: Activation and reaction energies corresponding to transition states and products for the 32CA reaction of 1-(4-nitrophenyl)-5H-pyrrolin-2-one **A2** and **A1** (meta, R=CH₃, OCH₃, (CH₃)₂N, Br, and NO₂) at the M06/6-311G (*d*, *p*) level of the theory in the gas phase for path A. All energies are in kcal/mol.

Substituents	Meta							
	TS1A-EXO	TS2A-ENDO	TS3A-EXO	TS4A-ENDO	P1A-EXO	P2A-ENDO	P3A-EXO	P4A-ENDO
H	4.5	10.6	9.6	7.6	-23.4	-20.4	-19.7	-20.3
<i>ERGs</i>								
CH ₃	2.5	10.4	—	7.2	-24.8	-20.6	-20.2	-20.8
OCH ₃	3.6	10.3	5.2	6.3	-27.6	-21.4	-21.4	-22.0
(CH ₃) ₂ N	-1.6	—	—	5.9	-28.4	-21.3	-21.9	-22.0
<i>EAGs</i>								
Br	3.7	11.7	9.1	8.1	-25.3	-20.3	-19.4	-20.3
NO ₂	3.8	13.1	—	9.6	-24.2	-19.4	-17.6	-21.0

whereas Table 3 shows substitution at the meta position. It ought to be stated that, after the exhaustive search to locate certain transition states, it proved futile. However, we believe it will not substantially affect the pattern we see based on the accumulated data. Tables 2 and 3 show that both ERGs and EAGs on **A1** favors the formation of the product where **A1** adds across the C=C olefin bond of the **A2**. The formation of **P1A-EXO** through **TS1A-EXO** is seen to be the most kinetically preferred pathway and the product is thermodynamically stable in all instances when both ERGs and EAGs are placed at both para and meta positions of **A1**. Due to the higher activation barriers of the transition states (**TS1B** and **TS2B**) and the thermodynamically unstable products (**P1B** and **P2B**) that are provided as seen in path B, the addition of **A1** across the C=O olefinic bond of **A2** can be ruled out. Hence, no substituents effect was explored for path B.

Table 2 shows that CH₃ and (CH₃)₂N on the para position of **A1** reduced the activation barriers by a margin of about 1.4 and 0.6 kcal/mol, respectively. Also, the products formed are thermodynamically stable. The substituents OCH₃ and NO₂ at the para positions of **A1** tend to increase the activation barriers by 4.7 and 0.6 kcal/mol, respectively, with the formation of stable products. However, when Br is placed in the para position, all the activation energy increases, but that of **TS1A-EXO**, which leads to **P1A-EXO**, reduces the activation barrier by 0.3 kcal/mol. Similar trends were observed for the substitution at the meta position of **A1** with the EAGs and ERGs, as shown in Table 3. The negative activation barrier obtained for **TS1A-EXO** (R=(CH₃)₂N) can be attributed to the inability of the level of the theory to describe the system very well, leading to the underestimation of the activation energy.

3.3. Effect of the Substituents on the Ethylene Derivative (A2) in the 32CA Reaction of 1-(4-Nitrophenyl)-5H-Pyrrolin-2-One (A2) and Diarylnitrone. This section explores the effect of the substituents on the 1-(4-nitrophenyl)-5H-pyrrolin-2-one. Herein, the nitrophenyl group of **A2** was replaced by H, CH₃, and COOEt. This study investigated how various small and bulky groups on **A2** also affect the reaction. Scheme 3 shows an updated scheme for the reaction studied. Table 4 shows the activation and reaction energies of the transition

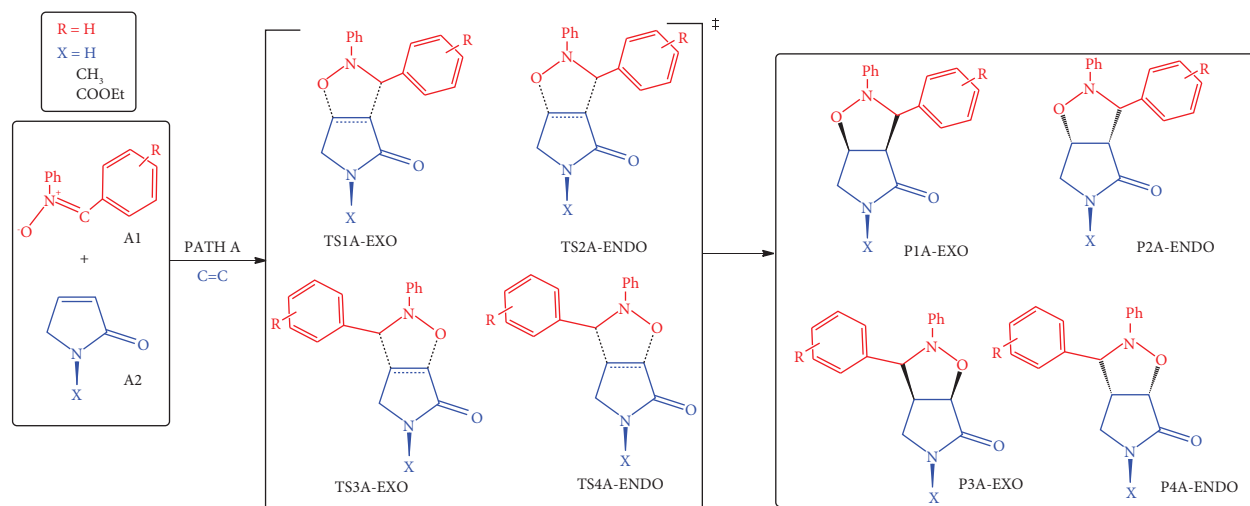
states and products of the 32CA reaction of **A1**(R=H) and **A2** (X=H, CH₃, and COOEt) explored.

As seen in Table 4, the formation of the “exo” product **P1A-EXO** through **TS1A-EXO** is still the favored reaction route. Activation barriers increased to 4.1 kcal/mol when a smaller group (**A2**, X=H) was used to form stable products. When X=CH₃, the activation barrier was reduced to 1.2 kcal/mol relative to when X=H. In the 32CA reaction of **A2** (X=COOEt) and **A1** (R=H), a bulkier group, on the other hand, reduced the activation barriers to about 0.1 kcal/mol of which the values obtained are close to the parent reaction. Therefore, bulkier groups on **A2** reduce the activation barrier of the transition state, which leads to the formation of the favored product.

3.4. Analysis of the 32CA Reaction of 1-(4-Nitrophenyl)-5H-Pyrrolin-2-One (A2) Derivatives and Diarylnitrone Derivatives with the Global Reactivity Indices. This section discusses the inherent reactivity and selectivity of the 32CA reaction of the diarylnitrone derivatives and 1-(4-nitrophenyl)-5H-pyrrolin-2-one derivatives. The computed global reactivity indices for the reaction are displayed in Tables 5 and 6. The electronic chemical potential (μ), chemical hardness (η), electrophilicity (ω), and the maximum charge transfer (ΔN_{\max}) [23] results are displayed in Tables 5 and 6. From Table 5 (para), the ω values of TAC derivatives are also in the order (CH₃)₂N < CH₃ < OCH₃ < Br < NO₂.

Table 5 shows the nucleophilic indices (*N*) [23, 24] designating the nucleophilicity ability of the various reactants. It is evident that **A1** (R=NO₂) has the lowest *N* value of 2.66 eV, making **A1** (R=NO₂) the poorest nucleophile, while **A1** (R=(CH₃)₂N) has the highest *N* value of 4.12 eV, making **A1** (R=(CH₃)₂N) the best nucleophile.

From Table 6 (meta), the ω values of TAC derivatives are also in the order (CH₃)₂N < OCH₃ < CH₃ < Br < NO₂. ERGs on the meta position of the diarylnitrone reduce the ω values, implying why **A1** acts as a nucleophilic specie. Table 6 also displays the computed nucleophilic indices (*N*) indicating the nucleophilic abilities of the various reactants. It is observed that **A1** (R=NO₂) has the lowest nucleophilicity value of 2.32 eV, making **A1** (R=NO₂) the poorest nucleophile, whereas **A1** (R=(CH₃)₂N) has the highest *N* value of 4.11 eV, making **A1** (R=(CH₃)₂N) the best nucleophile.



SCHEME 3: Proposed Scheme for 32CA reaction of diarylnitrones (A1) with substituents on the 1-(4-nitrophenyl)-5H-pyrrolin-2-one (A2).

TABLE 4: Activation and reaction energies corresponding to transition states and products for the 32CA reaction of **A2** (X=H, CH₃, and COOEt) and **A1** (R=H) at the M06/6-311G (*d*, *p*) level of the theory in the gas phase for path A. All energies are in kcal/mol.

Substituents	TS1A-EXO	TS2A-ENDO	TS3A-EXO	TS4A-ENDO	P1A-EXO	P2A-ENDO	P3A-EXO	P4A-ENDO
Ph-NO ₂	4.5	10.6	9.6	7.6	-23.4	-20.4	-19.7	-20.3
H	8.6	11.5	13.2	11.7	-24.2	-21.8	-20.7	-21.6
CH ₃	7.4	11.4	11.5	9.8	-25.2	-22.4	-21.2	-22.3
COOEt	4.4	11.0	9.8	8.5	-24.9	-20.2	-19.3	-20.0

TABLE 5: Global reactivity indices of diarylnitronone (TAC) with various substituents at the para position. Orbital energies are in eV.

Substrates	HOMO	LUMO	M	η	Ω	ΔN_{\max}	<i>N</i>
H	-6.08	-1.79	-3.94	4.29	1.80	0.92	3.28
CH ₃	-5.93	-1.71	-3.82	4.23	1.73	0.90	3.43
OCH ₃	-5.86	-1.73	-3.80	4.12	1.75	0.92	3.51
(CH ₃) ₂ N	-5.25	-1.38	-3.32	3.86	1.42	0.86	4.12
Br	-6.19	-1.99	-4.09	4.20	1.99	0.97	3.18
NO ₂	-6.71	-2.79	-4.75	3.92	2.87	1.21	2.66

TABLE 6: Global reactivity indices of diarylnitronone (TAC) with various substituents at the meta position. Orbital energies are in eV.

Substrates	HOMO	LUMO	μ	H	Ω	ΔN_{\max}	<i>N</i>
H	-6.08	-1.79	-3.94	4.29	1.80	0.92	3.28
CH ₃	-5.97	-1.72	-3.84	4.26	1.74	0.90	3.39
OCH ₃	-5.99	-1.67	-3.83	4.32	1.70	0.89	3.37
(CH ₃) ₂ N	-5.25	-1.46	-3.35	3.79	1.48	0.88	4.11
Br	-6.51	-2.21	-4.36	4.30	2.21	1.01	2.86
NO ₂	-7.05	-2.94	-5.00	4.10	3.04	1.22	2.32

4. Conclusion

The diarylnitronone moiety (**A1**) adds chemo- and regioselectively to the C=C olefinic bond over the C=O olefinic bond of 1-(4-nitrophenyl)-5H-pyrrolin-2-one (**A2**) to form a stereoselective cycloadduct, **P1A-EXO**, which is shown from the results obtained for this study. The reaction, therefore, proceeds through the proposed path A; thus, path A is kinetically favored over path B. The most kinetically favored reaction channel is the formation of **P1A-EXO**

through **TS1A-EXO** in support of the findings made by Muzychenko et al. Also, the formation of **P2A-ENDO** (-20.4 kcal/mol), **P3A-EXO** (-19.7 kcal/mol), and **P4A-ENDO** (-20.3 kcal/mol) are possible since their formation energies are thermodynamically stable and the activation barriers for the transition states, **TS2A-ENDO** (10.6 kcal/mol), **TS3A-EXO** (9.6 kcal/mol), and **TS4A-ENDO** (7.6 kcal/mol), are appreciably low; this goes on to favor the report of an “endo” approach of **A1** being possible by Muzychenko et al. However, **P1A-EXO** was isolated as

a major product since the rate constant for the formation of the preferred product **PIA-EXO** in the 32CA of diarylnitronone **A1** and 1-(4-nitrophenyl)-5H-pyrrolin-2-one **A2** is $3.1 \times 10^9 \text{ s}^{-1}$, which is about 182 times faster than the next competing pathway with a rate constant of $1.7 \times 10^7 \text{ s}^{-1}$. Irrespective of the electronic nature of the substituents on the para and meta positions of **A1**, the chemo-, regio-, and stereo-selectivities remained unchanged. Smaller and bulkier groups on **A2** maintain the trends of the chemo-, regio-, and stereo-selectivities of the reaction. However, the bulky groups tend to reduce the activation energies of the transition states that lead to the formation of the products. Future research should explore solvent effects on the mechanism of the (3 + 2) cycloaddition reaction of 1-(4-nitrophenyl)-5H-pyrrolin-2-one with other dipoles such as azides and nitrile oxides that may provide novel reaction routes to the formation of azoles and isoxazolines which possess antifungal, anti-inflammatory, and antibacterial properties.

Data Availability

The data used to support the findings of this study are available on request from the corresponding author.

Conflicts of Interest

The authors declare that there are no conflicts of interest.

Authors' Contributions

SA, JAK, and CHB conceived the idea and planned the study. SA ran computations and wrote the manuscript. JAK, RT, EA, and AA analyzed data. All the authors approved the manuscript before submission.

Acknowledgments

The authors are very grateful to the National Council for Tertiary Education, Republic of Ghana, for a research grant under the Teaching and Learning Innovation Fund (TALIF/KNUST/3/0008/2005) and South Africa's Centre for High-Performance Computing for access to additional computing resources on the lengau cluster.

Supplementary Materials

The zero-point corrected absolute energies and coordinates of all the computed structures reported herein are shown in Tables S1–S7 in the Supplementary file. The reported imaginary frequencies of the optimized transition states in the reaction of 1-(4-nitrophenyl)-5H-pyrrolin-2-one (**A2**) with diarylnitronone (**A1**, R=H) at the M06/6-311G (*d*, *p*) level of the theory in the gas phase at 25°C are presented in Tables S8. (*Supplementary Materials*)

References

- [1] E. A. Fosu, C. Obuah, L. Hamenu, A. Aniagyei, M. K. Ainooson, and K. K. Govender, "Quantum mechanistic studies of the oxidation of ethylene by rhenium oxo complexes," *Journal of Chemistry*, vol. 2021, Article ID 7931956, 11 pages, 2021.
- [2] A. A. Melekhova, A. S. Smirnov, A. S. Novikov, T. L. Panikorovskii, N. A. Bokach, and V. Y. Kukushkin, "Copper(I)-Catalyzed 1,3-dipolar cycloaddition of ketonitrones to dialkylcyanamides: a step toward sustainable generation of 2,3-Dihydro-1,2,4-oxadiazoles," *ACS Omega*, vol. 2, no. 4, pp. 1380–1391, 2017.
- [3] A. S. Kritchenkov, N. A. Bokach, M. Haukka, and V. Y. Kukushkin, "Unexpectedly efficient activation of push-pull nitriles by a PtII center toward dipolar cycloaddition of Z-nitrones," *Dalton Transactions*, vol. 40, no. 16, pp. 4175–4182, 2011.
- [4] A. I. Adjieufack, J. Moto Ongagna, A. Pouyewo Tenambo, E. Opoku, and I. N. Mbouombouo, "How a ctcc[3 + 2] cycloaddition reaction of *N*-substituted phenylnitrones with styrene: a molecular electron density theory analysis," *Organometallics*, vol. 41, no. 24, pp. 3809–3822, 2022.
- [5] M. A. Kinzhalov, A. S. Novikov, K. V. Luzyanin, M. Haukka, A. J. L. Pombeiro, and V. Y. Kukushkin, "Pd^{II}-mediated integration of isocyanides and azide ions might proceed via formal 1,3-dipolar cycloaddition between RNC ligands and uncomplexed azide," *New Journal of Chemistry*, vol. 40, no. 1, pp. 521–527, 2016.
- [6] A. I. Adjieufack, A. Gaudel-Siri, M. Gingras, and D. Siri, "Unraveling the reaction mechanism of AlCl₃ Lewis acid catalyzed acylation reaction of pyrene from the perspective of the molecular electron density theory," *New Journal of Chemistry*, vol. 47, no. 4, pp. 1925–1934, 2023.
- [7] M. L. Waters and W. D. Wulff, "The Synthesis of Phenols and Quinones via Fischer Carbene Complexes," *Organic Reactions*, vol. 70, pp. 121–623, 2008.
- [8] G. B. Pipim, R. Tia, and E. Adei, "Investigating the regio-stereo- and enantio-selectivities of the 1,3-dipolar cycloaddition reaction of C-cyclopropyl-N-phenylnitronone derivatives and benzyldenecyclopropane derivatives: a DFT study," *Journal of Molecular Graphics and Modelling*, vol. 100, Article ID 107672, 2020.
- [9] E. T. Pelkey, S. J. Pelkey, and J. G. Greger, "Reactions of 3-Pyrrolin-2-Ones," *Advances in Heterocyclic Chemistry*, Elsevier, , vol. 128, pp. 435–565, 2019.
- [10] A. I. Meyers, C. J. Andres, J. E. Resek, M. A. McLaughlin, C. C. Woodall, and P. H. Lee, "A rapid and efficient approach to chiral, nonracemic aza sugars from nonsugars. A formal synthesis of 1,4-Dideoxy-1,4-imino-d-lyxitol," *Journal of Organic Chemistry*, vol. 61, no. 8, pp. 2586–2587, 1996.
- [11] I. F. Cottrell, P. J. Davis, and M. G. Moloney, "Stereoselective oxygenation of bicyclic lactams," *Tetrahedron Asymmetry*, vol. 15, no. 8, pp. 1239–1242, 2004.
- [12] F. Fariña, M. V. Martín, M. C. Paredes, and A. Tito, "Pseudoesters and derivatives. XXV. 1,3-Dipolar cycloaddition of diazomethane to 5-methoxy-3-pyrrolin-2-ones," *Journal of Heterocyclic Chemistry*, vol. 24, no. 5, pp. 1269–1274, 1987.
- [13] W. J. Koot, H. Hiemstra, and W. N. Speckamp, "(R)-1-Acetyl-5-isopropoxy-3-pyrrolin-2-one: a versatile chiral dienophile from (S)-Malic acid," *Journal of Organic Chemistry*, vol. 57, no. 4, pp. 1059–1061, 1992.
- [14] N. Langlois, N. Van Bac, N. Dahuron et al., "1,3-Dipolar cycloadditions of nitrones to α,β -unsaturated γ -lactams derived from (S)-pyroglutaminol," *Tetrahedron*, vol. 51, no. 12, pp. 3571–3586, 1995.
- [15] G. F. Muzychenko, V. G. Kul'nevich, L. N. Zharkikh et al., "Synthesis of 3,6,7-triazabicyclo [3.3.0] octenes by 1,3-

- cycloaddition with N-arylpiperidin-2-ones,” *Chemistry of Heterocyclic Compounds*, vol. 28, no. 7, pp. 742–745, 1992.
- [16] J. Atta-Kumi, G. B. Pipim, R. Tia, and E. Adei, “Investigating the site-regio-and stereo-selectivities of the reactions between organic azide and 7-heteronorborene: a DFT mechanistic study,” *Journal of Molecular Modeling*, vol. 27, no. 9, p. 248, 2021.
- [17] G. B. Pipim, R. Tia, and E. Adei, “Quantum chemical investigation of the formation of spiroheterocyclic compounds via the (3 + 2) cycloaddition reaction of 1-methyl-3-(2,2,2-trifluoroethylidene) piperidin-2-one with diazomethane and nitrene derivatives,” *Tetrahedron*, vol. 94, Article ID 132306, 2021.
- [18] Y. Zhao and D. G. Truhlar, “Density functionals with broad applicability in chemistry,” *Accounts of Chemical Research*, vol. 41, no. 2, pp. 157–167, 2008.
- [19] M. J. Frisch, G. W. Trucks, H. B. Schlegel et al., “Gaussian 16, Revision A. 03, Gaussian,” *Inc., Wallingford CT*, vol. 3, 2016.
- [20] P. J. Hay, “Gaussian basis sets for molecular calculations. The representation of 3d orbitals in transition-metal atoms,” *The Journal of Chemical Physics*, vol. 66, no. 10, pp. 4377–4384, 1977.
- [21] A. J. H. Wachters, “Gaussian basis set for molecular wavefunctions containing third-row atoms,” *The Journal of Chemical Physics*, vol. 52, no. 3, pp. 1033–1036, 1970.
- [22] K. Raghavachari and G. W. Trucks, “Highly correlated systems. Excitation energies of first row transition metals Sc–Cu,” *The Journal of Chemical Physics*, vol. 91, no. 2, pp. 1062–1065, 1989.
- [23] L. R. Domingo, M. Ríos-Gutiérrez, and P. Pérez, “Applications of the conceptual density functional theory indices to organic chemistry reactivity,” *Molecules*, vol. 21, pp. 748–756, 2016.
- [24] A. Tawiah, G. B. Pipim, R. Tia, and E. Adei, “Exploring the chemo-regio-and stereoselectivities of the (3 + 2) cycloaddition reaction of 5,5-dimethyl-3-methylene-2-piperidinone with C, N-diarylnitrenes and nitrile oxide derivatives: a DFT study,” *Journal of Molecular Modeling*, vol. 27, no. 10, pp. 287–313, 2021.